Hydrogen molecules and chains in a superstrong magnetic field

Dong Lai, Edwin E. Salpeter, and Stuart L. Shapiro
Center for Radiophysics and Space Research, Space Sciences Building, Cornell University, Ithaca, New York, 14853
(Received 11 October 1991)

We study the electronic structures of hydrogen polymolecules H_n ($n=2,3,4,\ldots$) in a superstrong magnetic field ($B \gtrsim 10^{12}$ G) typically found on the surface of a neutron star. Simple analytical scaling relations for several limiting cases (e.g., large n, high B field) are derived. We numerically calculate the binding energies of H_n molecules for various magnetic-field strengths. For $n=2,3,4$ we employ a Hartree-Fock method to determine the ground-state structure of the molecule in the Born-Oppenheimer approximation. For $n=\infty$ (a bound infinite chain) we use a variational method. For a given magnetic-field strength, the binding energy per atom in the H_n molecule is found to approach a constant value as n increases. For typical field strengths of interest, energy saturation is essentially achieved once n exceeds 3 to 4. We also consider the structure of negative H ions in a high magnetic field. For $B \sim 10^{12}$ G the dissociation energy of an atom in a hydrogen chain and the ionization potential of H^- are smaller than the ionization potential of neutral atomic hydrogen.

PACS number(s): 32.60.+i, 97.10.Ld, 31.20.Di, 97.60.Jd

I. INTRODUCTION

The intense magnetic fields ($B \sim 10^{12}$ G) believed to exist on the surfaces of some neutron stars motivate the study of atoms, molecular chains, and condensed matter in fields of extreme magnitude (see Ref. [1] for an early general review). Moreover, the structure of matter in a strong magnetic field is an interesting problem of fundamental physics, as well as an important astrophysical issue in the context of neutron stars.

In superstrong magnetic fields the structure of atoms and condensed matter is dramatically changed by the fact that the magnetic force on an electron is stronger than the Coulomb force it experiences. In the direction perpendicular to the field, the electrons are confined to move on cylindrical Landau orbitals around a nucleus. The orbitals have radii

$$\rho_m = (2m+1)^{1/2}\hat{\rho}\ , \quad m=0,1,2,\ldots \tag{1.1}$$

where $\hat{\rho}$ is the cyclotron radius

$$\hat{\rho} = (\hbar c/eB)^{1/2} = 2.57\times 10^{-10} B_{12}^{-1/2}\ (\text{cm})\ , \tag{1.2}$$

and B_{12} is the magnetic-field strength in units of 10^{12} G. Because of this enormous confinement of electrons in the transverse direction by the magnetic field, the Coulomb force becomes much more effective for binding electrons in the parallel direction, thereby giving greatly increased binding energy. Furthermore, it is possible for these elongated atoms to form molecular chains by covalent bonding along the field direction. Several different approaches have been developed and some detailed calculations have been performed for determining the structure of atoms and one-dimensional infinite chains in a strong magnetic field. These methods include variational calculations [2–4], Thomas-Fermi-type statistical models [5,6], Hartree-Fock calculations [7–9], and density-functional calculations [10,11]. The general consensus is that for elements with $Z>4$, the isolated atom is energetically favored over the molecular chain for typical magnetic fields characterizing neutron-star surface. In particular, the infinite iron chain is not bound, a qualitatively different conclusion from the early result [3]. Therefore, the polar cap model for pulsar emission [12], which is based on the assumption of strong binding of the magnetic material ($E_b \gtrsim 3$ keV) to support a finite electric-field boundary condition, may have a problem.

For young radio pulsars, which cannot be accreting much gas and still remain visible as pulsars, one might expect the surface to consist mainly of condensed iron-peak elements formed at the neutron-star birth. But for accreting neutron stars, acquiring fresh material either from the interstellar medium or from a binary companion, one expects a gaseous atmosphere to form on the top of the surface. For these neutron stars, the light, accreted material should dominate the atmosphere and surface layers while the heavy elements sink down quickly due to gravitational separation [13]. In fact, because of the light material sitting on the surface, Fe may be transformed to other elements by electron capture, so the primordial Fe may not be present at all [14,15]. For these reasons, the lightest elements, like H and He, may be the most important species in a neutron-star atmosphere. If the temperature there is not too high, light atoms, molecules, and/or bound chains may form.

In the past, significant efforts have been devoted to the theoretical study of hydrogen atoms in a strong magnetic field. Accurate calculations of the energy levels of the H atom in a magnetic field of arbitrary strength have been performed (see, e.g., [16] and references therein). There have also been some variational calculations of molecular ions (H_2^+) in strong magnetic field [17,18] and a few investigations of H molecules in a strong field [19]. The errors in the atomic and molecular energies from these variational calculations are usually bigger than 10%, re-

sulting in an unreliable dissociation energy for the molecule. For the magnetic-field strengths of interest here, no reliable binding energies of H molecules have been obtained previously.

As a first step in understanding the local physical properties of a neutron-star atmosphere, we calculate in this paper the ground-state binding energies of several different forms of H in a strong, uniform magnetic field. Such forms include hydrogen polymolecules H_n ($n=2,3,4,\ldots$), infinite chains ($n=\infty$), molecular ions (H_2^+), and negative ions (H^-), the latter being of potential importance for the opacities of a neutron-star atmosphere. We focus entirely on the strong-field (but nonrelativistic) regime $B \gg 10^9$ G, for which the cyclotron energy of an electron is much larger than the Coulomb energy (see Sec. II). In all of our calculations, we use the standard Born-Oppenheimer approximation, ignoring possible corrections to the energy due to finite proton mass [20]. Also, in our calculations of the molecules, we assume that the directions of the molecular axis and magnetic field coincide, corresponding to the molecular ground state. One can expect vibration (precession) of the molecular axis about (around) the magnetic-field axis, giving rise to possible rovibrational molecular spectra, but we consider only the molecular ground state. We calculate the binding energies for $n=2,3,4$ by solving the Hartree-Fock (HF) equations for the electrons. As n increases, the single-determinant Hartree-Fock method becomes invalid because of the mixing of different configurations. Fortunately, for a given B field, the binding energy per atom approaches a constant independent of n ("saturation") at $n \sim 3,4$ for typical field strengths of interest, as we demonstrate analytically. Qualitatively, this saturation occurs because as n increases, it becomes energetically more favorable to have more electrons occupy the same inner Landau orbitals rather than have each of them occupy different nodeless Landau orbitals. Our numerical results confirm our qualitative picture. We calculate the binding energy for the infinite H chain using a variational method. The variational method is essentially that of Flowers *et al.* [3] (which contains numerical errors as pointed out by Müller [4]), but our equations are derived from the energy functionals given by Neuhauser *et al.* [9]. Our approximate variational calculation proves to be quite good for the He chain when compared to more detailed Hartree-Fock calculations [9]. Therefore, we expect that our results are even better for H, where our approximations are more reliable and where no previous calculations have been performed.

The paper is organized as follows. Section II is a brief review of some basic concepts about atomic structures in a high magnetic field, including a discussion of the binding energy of negative H ions. In Sec. III we consider some qualitative features of molecules in a strong magnetic field and derive some simple scaling relations for the binding energies of molecules. In Sec. IV we discuss the methods and key equations used in our numerical calculations for H_n molecules ($n=2,3,4$ and $n=\infty$). In Sec. V we present our numerical results and confirm our qualitative picture of saturation. In Sec. VI we summarize our main conclusions.

II. BASIC CONCEPTS: ATOMS IN A STRONG MAGNETIC FIELD

In this section we review some basic concepts about atomic structure in a high magnetic field. These serve to introduce some useful terms and are important for understanding the molecular calculations performed below and the associated scaling relations. Our symbols for expressing the strength of magnetic field are as follows: B represents the magnetic-field strength in Gauss, b gives the magnetic field in atomic unit (a.u.), i.e., $b=B/B_0$, where

$$B_0=m_e^2e^3c/\hbar^3=2.35\times10^9 \text{ G} ;$$

B_{12} gives the field strength in 10^{12} G, i.e., $B_{12}=B/(10^{12}$ G). Recall that in atomic units, energy is expressed in units of

$$e^2/a_0=2 \text{ Ry}=2\times13.6 \text{ eV} ,$$

and length is in units of Bohr radius

$$a_0=\hbar^2/m_ee^2=0.529\times10^{-8} \text{ cm} .$$

For a free electron in an uniform magnetic field, the motion perpendicular to the field is quantized into different Landau levels, with the Landau excitation energy (the cyclotron energy) given by [21]

$$\hbar\omega_e=\hbar\frac{eB}{m_ec}=b \text{ (a.u.)}=11.57B_{12} \text{ (keV)} . \tag{2.1}$$

The ground-state ($n_L=0$) Landau wave functions are given in cylindrical coordinates (ρ,z,ϕ) by

$$W_{0m}(\rho,\phi)=\frac{1}{\sqrt{2\pi m!}}\left[\frac{\rho}{\sqrt{2}}\right]^m e^{-\rho^2/4}e^{-im\phi} . \tag{2.2}$$

Here the B fields lies along the z direction and, for the subscripts in $W_{n_L,m}$, n_L is the Landau-level quantum number (the number of nodes in the ρ direction), while m is the negative of the angular momentum in the z direction. In Eq. (2.2), the length is in the units of the cyclotron radius

$$\hat{\rho}=\left[\frac{\hbar c}{eB}\right]^{1/2}=b^{-1/2}\text{(a.u.)}=2.57\times10^{-10}B_{12}^{-1/2} \text{ (cm)} . \tag{2.3}$$

Accordingly, the electron distribution has a maximum at

$$\rho_m=(2m+1)^{1/2}\hat{\rho} , \quad m=0,1,2,\ldots . \tag{2.4}$$

These values are the radii of the Landau orbitals perpendicular to the field. Note that the energy of a free electron does not depend on m at all; for $m \gg 1$ the maximum in the ρ distribution at ρ_m is very sharp. The electrons move as free particles in the z direction.

For an extremely strong magnetic field,

$$B \gtrsim B_{\text{rel}}=m_e^2c^3/\hbar e=(\hbar c/e^2)^2B_0=4.414\times10^{13} \text{ G} ,$$

the electron cyclotron energy becomes comparable to the electron rest mass energy and the transverse motion of

the electron becomes relativistic [21,22]. In this regime, our nonrelativistic calculations will not be strictly valid. But relativistic effects should not qualitatively change our results, since the corrections are only of order $(v_z/c)^2 \sim |E|/m_e c^2$ (v_z is the electron speed in the z direction and $|E|$ is the binding energy), which is much less than unity for light elements. For practical applications we are interested only in the field strengths up to a little more than $B_{\rm rel}$; for pedagogical purposes we shall consider arbitrarily large B but shall use the nonrelativistic equations throughout.

Now we consider the energies of atoms. If the magnetic field is sufficiently strong so that

$$\frac{Ze^2}{\hat{\rho}} \ll \hbar\omega_e \ , \quad \text{or} \quad \hat{\rho} \ll \frac{a_0}{Z} \ , \tag{2.5}$$

i.e.,

$$b \gg Z^2 \tag{2.6}$$

(Z is the ion charge), then the Coulomb potential can be treated as a perturbation, and electrons are confined to the ground Landau level ("adiabatic approximation"). For light atoms and typical field strengths found on the surface of a neutron star, this condition is well satisfied. We restrict our attention to this high magnetic-field regime throughout this paper, i.e., all electrons will be in the $n_L=0$ state, so we will henceforth omit the index n_L. Electrons in the ground Landau level have spins all aligned antiparallel to the magnetic field; hence, we can ignore the electron spin degree of freedom completely. Within this adiabatic approximation, the transverse wave functions of electrons are fixed to be the Landau wave functions, while the electrons adjust themselves in the z direction. The electrons are then described by a one-dimensional Schrödinger equation (or HF equations) in z, with the electric potential averaged over the transverse direction and weighted by Landau wave functions. Calculations of hydrogen atomic structure that do not employ this simplification have been performed (e.g., [16]).

Let us consider the energy spectrum of a hydrogenic atom (one electron, nuclear charge Z). The electron wave functions may be written as $\Phi_{m\nu}=W_m(\mathbf{r}_\perp)f_{m\nu}(z)$, where ν denotes the number of nodes in f. Substituting this function into the Schrödinger equation and averaging over the transverse direction yields a one-dimensional Schrödinger equation for f:

$$-\frac{\hbar^2}{2m_e\hat{\rho}^2}f''_{m\nu}-\frac{Ze^2}{\hat{\rho}}V_m(z)f_{m\nu}=E_{m\nu}f_{m\nu} \ , \qquad m,\nu=0,1,2,\ldots \ . \tag{2.7}$$

The averaged potential is given by

$$V_m(z)=\int d^2\mathbf{r}_\perp |W_m(\mathbf{r}_\perp)|^2\frac{1}{r} \ . \tag{2.8}$$

Hereforth we shall employ $\hat{\rho}$ as our length unit in all the wave functions and averaged potentials, making them dimensionless functions. It is important to distinguish two distinct types of excitations in the energy spectrum $E_{m\nu}$. The "deep-bound" states have no nodes in their z wave functions ($\nu=0$). Their energies are approximately given by [1]

$$E_{m0-} \simeq -2AZ^2 l_m^2 \ \text{(a.u.)} \ , \qquad l_m=\ln\left[\frac{1}{Z\rho_m}\right]=\ln\left[\frac{1}{Z}\left[\frac{b}{2m+1}\right]^{1/2}\right] \ , \qquad m=0,1,2,\ldots \tag{2.9}$$

where A is of order unity. The sizes in atomic units of the atomic wave functions perpendicular and parallel to the field are, respectively,

$$R\sim\rho_m=\left[\frac{2m+1}{b}\right]^{1/2} \ , \quad L_z\sim\frac{1}{Zl_m} \ . \tag{2.10}$$

This excitation, which consists in changing a Landau orbital from m to $m+1$, enters only logarithmically into the electron binding energy, and therefore it is small. For hydrogen ($Z=1$) there is only one dimensionless parameter $b \gg 1$, but b has to become extremely large before asymptotic solutions are approached accurately. In the limit of the inequality $b \gg (\ln b)^2 \gg 1$ becoming very strong, and for m satisfying the double inequality $b/(\ln b)^2 \gg m \gg 1$, the asymptotic value of A in Eq. (2.9) is $A=1$. One may see this result by replacing the averaged potential $V_m(z)$ by $1/(|z|+\rho_m)$ as B becomes increasingly large; the analytic solution of the Schrödinger equation for this potential gives $A=1$ asymptotically [23]. Our numerical solutions of the Schrödinger equation (2.7) gives $A\sim 0.3$ for $B_{12}\sim 1$ and A is still only ~ 0.5 even for $B_{12}\sim 10^4$. In the asymptotic regime, the energy difference Δ between states m and $m+1$ is only

$$\Delta \simeq (\ln b)\ln\left[\frac{2m+3}{2m+1}\right] \ \text{(a.u.)} \ , \tag{2.11}$$

much smaller than the ground-state binding energy of $0.5(\ln b)^2$ (a.u.).

Another type of excitation consists in having nodes in the z wave functions ($\nu\neq 0$). These states are only weakly bound, e.g., the $\nu=1$ state (for $Z=1$) has about the same binding energy as the ground state of a normal magnetic-free H atom, $E\simeq -13.6$ eV, since the equation describing this odd-parity state is almost the same as the radial equation satisfied by the s state in a normal hydrogen atom [1,23].

Now we consider heavy atoms. When $a_0/Z \gg \sqrt{2Z+1}\hat{\rho}$, i.e., $b \gg 2Z^3$ (superstrong fields), all electrons settle into the deep-bound levels with $m=0,1,2,\ldots,Z-1$. The atomic energy is approximately given by the sum of all the eigenvalues of Eq. (2.9). Accordingly, we can obtain an asymptotic expression for the total energy of the atom for $Z \gg 1$ [24]

$$E\sim -Z^3 l^2 \ , \quad l=\ln\left[\frac{a_0}{Z\sqrt{2Z+1}\hat{\rho}}\right]\simeq\ln\left[\frac{b}{2Z^3}\right]^{1/2} \qquad \text{for } l\gg 1 \ . \tag{2.12}$$

When $Z^{4/3} \ll b \ll 2Z^3$ (intermediate-strong fields, but still high enough to ignore the Landau excitation), the

inner Landau orbitals are populated by many electrons. In this regime the electrons can be treated as a one-dimensional Fermi gas in a more or less spherical atomic cavity [25]. Simple dimensional analysis for this gas gives for the electron density $n_e \sim bp_F$ (recall the degeneracy of a Landau level is $eB/hc \sim b$) and for the kinetic energy density $\varepsilon_k \sim bp_F^3$, where p_F is the Fermi momentum. Thus the total kinetic energy is $E_k \sim R^3 n_e^3/b^2 \sim Z^3/b^2R^6$, where R is the atomic radius. The potential energy is $E_p \sim -Z^2/R$. Therefore, the atomic energy is

$$E \sim \frac{Z^3}{b^2R^6} - \frac{Z^2}{R} . \tag{2.13}$$

Minimization of E with respect to R gives

$$R \sim Z^{1/5}b^{-2/5} \text{ (a.u.)} , \quad E \sim -Z^{9/5}b^{2/5} \text{ (a.u.)} . \tag{2.14}$$

More detailed Thomas-Fermi-type models have been developed for this regime [5,6,26], giving approximately the same scaling relations. We shall see below that, in a certain limit, the binding energy per atom as a function of magnetic-field strength in a molecule is very similar to that found in a heavy atom.

Consider next the possibility of one or more electrons being attached to a neutral hydrogen atom to form negative hydrogen ions. First imagine the formation of a H^- ion by attaching an "extra" electron to a H atom in the ground state with $m=0$. The extra electron can only settle into the $m=1$ state, which, if we ignore the screening of the proton potential due to the first ($m=0$) electron, has a binding energy of $|E_{10}|$ as in Eq. (2.9) with $Z=1$. But there is Coulomb repulsion between the two electrons, which reduces the binding of the $m=1$ electron. The repulsive energy is of order $(\ln\sqrt{b})/L_z$, which is of the same order as $|E_{10}|$. But the repulsive energy is smaller $|E_{10}|$ because of the cylindrical charge distribution of both electrons. Therefore, H^- is bound relative to $H+e$ and its ionization potential is also proportional to $(\ln\sqrt{b})^2$.

More detailed variational calculations have been performed for a Z ion (nuclear charge Z) with n electrons in a superstrong-field regime [24]. The sizes of the ion perpendicular and parallel to the field are, respectively,

$$R \sim \rho_{n-1} = \left[\frac{2n-1}{b}\right]^{1/2} , \quad L_z \sim \frac{1}{Zl} \quad \text{with } l = \ln\left[\frac{L_z}{R}\right] . \tag{2.15}$$

The ground-state energy of the ion is

$$E \simeq -\frac{n}{8}l^2(4Z-n+1)^2 . \tag{2.16}$$

Applying this result for hydrogen ions ($Z=1$), we see that the ionization potential of H^- to $H+e$ is $\sim\frac{1}{10}$ of the binding energy of the H atom. Also we see that for $n>2$, the negative ion $H^{-(n-1)}$ is not bound. Hence it is likely that the only possible bound negative H ion is H^-.

III. H_n: QUALITATIVE OVERVIEW AND SATURATION

Here we consider some qualitative features of H_n molecules (n is the number of atoms in the molecule) in a high magnetic field and derive simple scaling relations which apply in some limiting regimes. The fundamental difference between the normal H molecule in a zero B field and a molecule in a high magnetic field involves their different electronic structures. In the zero-field case, two H atoms in their ground states with spins opposite to each other form a H_2 molecule by covalent bonding. In this case adding more H atoms is not possible by the exclusion principle (unless one excites the third atom to an excited state, but the resulting H_3 is presumably short lived). In a high magnetic field, the spins of the electrons in the atoms are all aligned antiparallel to the magnetic field, and therefore two atoms in their ground states cannot bind together according to the exclusion principle. Instead, in a high magnetic field, one of the atoms has to be excited to a higher state first (which costs "activation energy") before the two atoms can form a molecule. However, as we discussed in Sec. II, exciting an electron in the H atom from Landau orbital m to $m+1$ costs very little energy, and therefore the resulting molecule is stable. In this way, more atoms can be added to form a bigger molecule, in contrast to the field-free case.

We now derive some approximate scaling relations. Let a be the atomic spacing (assuming equal spacing) and R be the radius of the molecule perpendicular to the field. Let the size of the molecule in the z direction be $L_z \sim na$. We consider $n \gg 1$ so that any edge effects may be ignored. As long as $L_z \gg R$, the Coulomb energy per atom of the molecule is always

$$U = -\frac{1}{a}\left[\ln\left[\frac{2a}{R}\right] + c\right] , \tag{3.1}$$

where c is approximately constant of order unity (see, e.g., [1] or Appendix A). We shall find it useful to define a "critical number" n_s by

$$n_s \equiv [b/(\ln b)^2]^{1/5} . \tag{3.2}$$

As in Sec. II, b has to be extremely large for asymptotic results to be accurate and for the analytical relations in this section, we assume $n_s \gtrsim 10$, which requires $b \gtrsim 5 \times 10^7$.

Let us consider the case when all electrons in the molecule occupy the deep-bound states with $m=0,1,2,\ldots,n-1$. We shall see that this regime requires $n_s \gg n \gg 1$ and shall refer to it as the regime "before saturation." The molecule has a cylindrical shape, with the cylinder radius given by

$$R \sim \sqrt{2n-1}\hat{\rho} \sim \left[\frac{2n}{b}\right]^{1/2} \text{ (a.u.)} . \tag{3.3}$$

Each electron fills the entire length of the cylinder, L_z. Accordingly, the kinetic energy of an electron is $\sim 1/L_z^2$. Using Eq. (3.1), the energy per atom is then

$$E \sim \frac{1}{L_z^2} - \frac{n}{L_z} l$$

$$\text{with } l = \ln\left[\frac{2a}{R}\right] = \ln\left[\frac{2^{1/2} L_z b^{1/2}}{n^{3/2}}\right], \quad (3.4)$$

where we have assumed $l \gg 1$. Variation of E with respect to L_z gives

$$E \sim -n^2 l^2, \quad L_z \sim \frac{1}{nl}$$

$$\text{with } l \simeq \ln\left[\frac{2^{1/2}}{l}\frac{n_s^{5/2}}{n^{5/2}}\right] \sim \tfrac{5}{2}\ln\left[\frac{n_s}{n}\right]. \quad (3.5)$$

As mentioned, this scaling behavior is expected to be correct in the regime $n_s \gg n \gg 1$, so that $l \gg 1$. For the H_2 molecule, $n=2$, the dissociation energy should be comparable to the ionization potential of the hydrogen atom for sufficiently large fields: They should both scale like $(\ln b)^2$, but we shall see that their ratio approaches a constant only for $b \gg 10^7$. In this regime, the binding energy of the molecule $-nE \propto n^3$. We notice the similarity between Eq. (2.12) for the energy of heavy atoms in the superstrong field and Eq. (3.5) for molecular energy before saturation. We present a more detailed variational calculation for this regime in Appendix A, where we get the coefficients for the relations above.

For a given B field, as n increases, the electrons occupy more and more nodeless Landau orbitals (up to $m = n-1$); beyond the critical number n_s, it becomes energetically more favorable for electrons to settle into the inner Landau orbitals with nodes in their z wave functions. Beyond this point saturation occurs, as the energy per atom asymptotes to a value independent of n, as we now show. The saturation point is reached once $a \sim R$, which is equivalent to $n \sim n_s$.

After saturation, many electrons settle into the $\nu \neq 0$ states, and the electrons can be treated as a Fermi sea in the z direction. In order of magnitude, the electrons occupy states with $m = 0,1,2,\ldots,n_s-1$ and $\nu = 0,1,2,\ldots,n/n_s$. For $n \gg n_s \gg 1$, we can approximate the electron distribution in the molecule to be a uniform cylinder with radius R and atomic spacing a. The distribution is uniform because in the transverse direction the area covered by the m orbitals increases roughly as $(\sqrt{2m+1})^2 \propto m$. Hence the volume increases with the number of interior electrons, giving a constant electron density. Note that the cylinder must have a reasonably sharp edge because the wave function described by Eq. (2.2) has such a sharp maximum at ρ_m. The energy per atom is then

$$E = \frac{2\pi^2}{3R^4 a^2 b^2} - \frac{1}{a}\left[\ln\left[\frac{2a}{R}\right] - (\gamma - \tfrac{3}{4})\right],$$

$$\gamma = 0.577\ldots, \quad (3.6)$$

where the first term is the kinetic energy and the second term is the Coulomb energy (the Madelung energy for the one-dimensional uniform lattice [27]). We can minimize the energy by varying a and R independently, giving

$$R = 1.70 b^{-2/5}, \quad a = 1.88R, \quad E = -0.390 b^{2/5}. \quad (3.7)$$

These scaling results become increasingly more reliable as n increases beyond n_s, i.e., $n \gg n_s \gg 1$. E is independent of n in this regime. Note that this scaling behavior for a molecule beyond saturation is the same as that for a heavy atom in a field of intermediate strength.

The above relations provide qualitative understanding of the molecular binding energy as a function of n and the magnetic-field strength. But for these scaling laws to apply accurately, we need $b \gg 10^7$, i.e., $B_{12} \gg 10^4$. Such high field strengths are not to be found on neutron-star surfaces. Nevertheless, the scaling behavior derived above and the onset of saturation is confirmed by the detailed calculations reported below.

IV. CALCULATION OF H_n MOLECULES

In this section we discuss our detailed calculations of H_n molecules in a superstrong magnetic field. Specifically, we calculate the ground-state binding energy of small H molecules ($n=2,3,4$) and that of an infinite H chain ($n=\infty$). In both cases we adopt the Born-Oppenheimer approximation (ignoring any finite proton mass effects on the electronic energy) by fixing the atomic spacing a, calculating the resulting electronic structure, and finding the minimum energy as a function of a. Since the methods adopted for these two cases are otherwise quite different, we discuss them separately.

A. Small molecules before saturation

We now present our equations for the simplest molecule H_2 ($n=2$). Corresponding equations for the higher n's can easily be generated (see, e.g., Appendix B).

1. H_2: Molecular-orbital method (MO)

For a many-electron system in a high magnetic field, the general one-electron basis wave functions are of the form

$$\Phi_{m\nu}(\mathbf{r}) = W_m(\rho,\phi) f_{m\nu}(z). \quad (4.1)$$

In writing Eq. (4.1), we omit the subscript $n_L=0$ in W since all electrons are in the ground Landau level (see Sec. II); ν denotes the quantum number for the z-dependent wave function f (ν is the number of nodes of f in the z direction). For a small number of electrons (i.e., before saturation) we can set $\nu=0$ since the high-ν states have much higher energies compared with the deep-bound states (see Sec. II) (however, we shall see in Sec. IV A 3 that at large atomic separations the ground state must include appreciable contributions from $\nu \neq 0$ basis functions). For two electrons, we can choose two orbitals,

$$\Phi_{00}(\mathbf{r}) = W_0(\rho,\phi) f_{00}(z), \quad \Phi_{10}(\mathbf{r}) = W_1(\rho,\phi) f_{10}(z). \quad (4.2)$$

The Hamiltonian for H_2 is

$$H=H_0(1)+H_0(2)+\frac{e^2}{r_{12}}+\frac{e^2}{a}\ , \tag{4.3}$$

with

$$\begin{aligned} H_0(1)&=-\frac{\hbar^2}{2m_e}\frac{\partial^2}{\partial Z_1^2}-\frac{e^2}{r_{A1}}-\frac{e^2}{r_{B1}}\ , \\ H_0(2)&=-\frac{\hbar^2}{2m_e}\frac{\partial^2}{\partial Z_2^2}-\frac{e^2}{r_{A2}}-\frac{e^2}{r_{B2}}\ , \end{aligned} \tag{4.4}$$

where 1,2 denote the electrons, A,B denote the ions, a is the distance between the two ions, r_{A1} is the distance between electron 1 and ion A, etc. (Fig. 1). As an approximation, we can choose the two orbitals to be solutions for the H_2^+ ion (the so-called molecular orbitals; see, e.g., [28]). Hence they satisfy

$$H_0\Phi_{m0}=\varepsilon_{m0}\Phi_{m0}\ ,\quad m=0,1\ . \tag{4.5}$$

Therefore, we can easily determine the f's by solving the one-dimensional Schrödinger equation

$$-\frac{\hbar^2}{2m_e\hat{\rho}^2}f''_{m0}-\frac{e^2}{\hat{\rho}}\tilde{V}_m(z)f_{m0}=\varepsilon_{m0}f_{m0}\ ,\quad m=0,1 \tag{4.6}$$

obtained by averaging the three-dimensional Schrödinger equation for Φ over the transverse direction. Equations (4.6) are solved for f's, subject to the boundary conditions

$$f'_{m0}=0\ \text{ at } z=0 \tag{4.7}$$

and

$$f_{m0}\to\exp\left[-|z|\left[\frac{2m_e\hat{\rho}^2}{\hbar^2}|\varepsilon_{m0}|\right]^{1/2}\right]\ \text{ as } |z|\to\infty\ . \tag{4.8}$$

The averaged potential is given by

$$\begin{aligned} \tilde{V}_m(z)&=\int d^2\mathbf{r}_\perp|W_m(\mathbf{r}_\perp)|^2\left[\frac{1}{r_A}+\frac{1}{r_B}\right] \\ &=V_m\left[z-\frac{a}{2}\right]+V_m\left[z+\frac{a}{2}\right]\ , \end{aligned} \tag{4.9}$$

where $V_m(z)$ is defined by Eq. (2.8). The two-electron wave function is then

$$\begin{aligned} \Psi(\mathbf{r}_1,\mathbf{r}_2)&=S[\Phi_{00}\Phi_{10}] \\ &=\frac{1}{\sqrt{2}}[\Phi_{00}(\mathbf{r}_1)\Phi_{10}(\mathbf{r}_2)-\Phi_{00}(\mathbf{r}_2)\Phi_{10}(\mathbf{r}_1)]\ , \end{aligned} \tag{4.10}$$

where the notation $S[\ ]$ denotes an antisymmetrized wave function. Therefore, the energy of H_2 is

$$\begin{aligned} E&=\langle\psi|H|\psi\rangle \\ &=\frac{e^2}{a}+\varepsilon_{00}+\varepsilon_{10}+E^{\rm dir}+E^{\rm exch}\ , \end{aligned} \tag{4.11}$$

where $E^{\rm dir}$ and $E^{\rm exch}$ are the direct and exchange energies, respectively. They are given by

$$\begin{aligned} E^{\rm dir}&=\int d^3\mathbf{r}_1d^3\mathbf{r}_2|\Phi_{00}(\mathbf{r}_1)|^2|\Phi_{10}(\mathbf{r}_2)|^2\frac{e^2}{r_{12}} \\ &=\frac{e^2}{\hat{\rho}}\int dz_1dz_2f_{00}(z_1)^2f_{10}(z_2)^2D_{01}(z_1-z_2) \end{aligned} \tag{4.12}$$

and

$$\begin{aligned} E^{\rm exch}&=-\int d^3\mathbf{r}_1d^3\mathbf{r}_2\Phi_{00}(\mathbf{r}_1)\Phi_{10}(\mathbf{r}_2)\Phi_{00}^*(\mathbf{r}_2)\Phi_{10}^*(\mathbf{r}_1)\frac{e^2}{r_{12}} \\ &=-\frac{e^2}{\hat{\rho}}\int dz_1dz_2f_{00}(z_1)f_{10}(z_2) \\ &\quad\times f_{00}(z_2)f_{10}(z_1)E_{01}(z_1-z_2)\ . \end{aligned} \tag{4.13}$$

In Eqs. (4.12) and (4.13), the direct and exchange kernels are defined by

$$D_{01}(z_1-z_2)=\int d^2\mathbf{r}_{1\perp}d^2\mathbf{r}_{2\perp}|W_0(\mathbf{r}_{1\perp})|^2|W_1(\mathbf{r}_{2\perp})|^2\frac{1}{r_{12}}\ , \tag{4.14}$$

$$\begin{aligned} E_{01}(z_1-z_2)&=\int d^2\mathbf{r}_{1\perp}d^2\mathbf{r}_{2\perp}W_0(\mathbf{r}_{1\perp})W_1(\mathbf{r}_{2\perp}) \\ &\quad\times W_0^*(\mathbf{r}_{2\perp})W_1^*(\mathbf{r}_{1\perp})\frac{1}{r_{12}}\ , \end{aligned} \tag{4.15}$$

where the adopted length unit in W is $\hat{\rho}$.

(For some useful mathematical relations for calculating the functions V_m, $D_{mm'}$, and $E_{mm'}$, see Appendix C.)

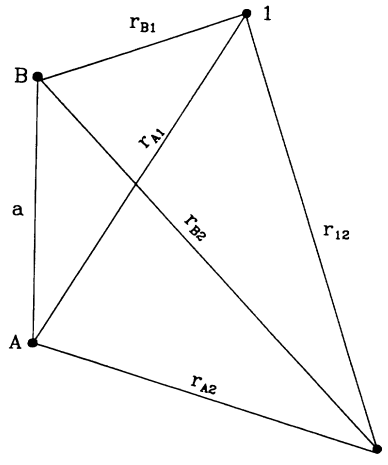

FIG. 1. The adopted coordinate system for a H_2 molecule in a high magnetic field.

2. H_2: Hartree-Fock method (HF)

Here the basis functions are the same as in the molecular-orbital method, but the f's are not given by the orbitals of H_2^+. Instead, we determine the f's self-consistently (see Appendix B), which yields the corresponding Hartree-Fock equations (we omit the index $\nu=0$) in this section):

$$\left[-\frac{\hbar^2}{2m_e}\frac{d^2}{dz^2}-\frac{e^2}{\hat{\rho}}\tilde{V}_m(z)+\frac{e^2}{\hat{\rho}}K_m(z)-\varepsilon_m\right]f_m(z)$$
$$=\frac{e^2}{\hat{\rho}}J_m(z)\ ,\quad m=0,1\ . \tag{4.16}$$

In Eq. (4.16), $\tilde{V}_m$ is again given by Eq. (4.9), the direct and exchange potentials K and J are given by

$$K_0(z)=\int dz' f_1(z')^2 D_{01}(z-z')\ , \tag{4.17}$$

$$J_0(z)=f_1(z)\int dz' f_1(z')f_0(z')E_{01}(z-z')\ , \tag{4.18}$$

and similarly for K_1 and J_1, where D_{01} and E_{01} are given by Eqs. (4.14) and (4.15). Boundary conditions for the f's are given by Eqs. (4.7) and (4.8). Similar equations have been derived in [7–9] and used to solve the structure of a single atom. The total energy of the molecule is then

$$E=\frac{e^2}{a}+\varepsilon_0+\varepsilon_1-E^{\rm dir}-E^{\rm exch}\ , \tag{4.19}$$

which just differs from Eq. (4.9) by the signs in front of the direct and exchange energy terms. The Hartree-Fock equations for general H_n molecules are given in Appendix B.

3. H_2: Configuration interaction

At large atomic separation a, the total energy of the molecule (excluding the e^2/a term) should approach the sum of the energies of two isolated atoms, one is the ground state, another in the first excited state (see Sec. III). The two methods above (MO and HF) do *not* give a correct large-a behavior for the total energy (see Fig. 2). This erroneous behavior is not surprising: As the ion separation increases, the electron orbitals employed above do not approach two separated orbitals of isolated atoms. A second electron configuration, which has a much higher energy than the first for small separation, but becomes more and more degenerate with the first configuration at large separation, must also contribute to the ground-state energy at large separation. At large separation, the calculations discussed above, which are based on a single-electron configuration, are clearly invalid due to the mixing between different configurations. To treat the molecule properly when the separation is large, we should include another configuration which consists of a single node state ($v\neq 0$) in our basis trial functions (the so-called configuration interaction; see [28]). To show that we can get the correct large-a behavior for the total energy, let us consider H_2. In Sec. IV A 1 our trial function is

$$\Psi_1=S[\Phi_{00}\Phi_{10}]\ . \tag{4.20}$$

In general, another configuration will be mixed with Ψ_1:

$$\Psi_2=S[\Phi_{01}\Phi_{11}]\ . \tag{4.21}$$

Notice that both configurations have the same symmetry with respect to the Hamiltonian: the total orbital angular momentum along the z direction is $M_{Lz}=1$, the total spin is $M_{Sz}=-1$, and both are even with respect to the operation $\mathbf{r}_i\rightarrow-\mathbf{r}_i$. In ordinary molecular notation, both are designated $^3\Pi_g$. At small separation, Ψ_2 lies much higher in energy than Ψ_1, so that when calculating the ground-state energy, we can simply employ Ψ_1. But at large separation, the energy of Ψ_2 is close to Ψ_1, and the mixing between these two configurations becomes important. We then have

$$H_{11}=\langle\Psi_1|H|\Psi_1\rangle=\frac{e^2}{a}+\varepsilon_{00}+\varepsilon_{10}+\frac{e^2}{\hat{\rho}}\int dz_1dz_2 f_{00}(z_1)^2f_{10}(z_2)^2D_{01}(z_1-z_2)$$
$$-\frac{e^2}{\hat{\rho}}\int dz_1dz_2 f_{00}(z_1)f_{10}(z_2)f_{00}(z_2)f_{10}(z_1)E_{01}(z_1-z_2)\ , \tag{4.22}$$

$$H_{22}=\langle\Psi_2|H|\Psi_2\rangle=\frac{e^2}{a}+\varepsilon_{01}+\varepsilon_{11}+\frac{e^2}{\hat{\rho}}\int dz_1dz_2 f_{01}(z_1)^2f_{11}(z_2)^2D_{01}(z_1-z_2)$$
$$-\frac{e^2}{\hat{\rho}}\int dz_1dz_2 f_{01}(z_1)f_{11}(z_2)f_{01}(z_2)f_{11}(z_1)E_{01}(z_1-z_2)\ , \tag{4.23}$$

$$H_{12}=\langle\Psi_1|H|\Psi_2\rangle=\frac{e^2}{\hat{\rho}}\int dz_1dz_2 f_{00}(z_1)f_{01}(z_1)f_{10}(z_2)f_{11}(z_2)D_{01}(z_1-z_2)$$
$$-\frac{e^2}{\hat{\rho}}\int dz_1dz_2 f_{00}(z_1)f_{11}(z_1)f_{10}(z_2)f_{01}(z_2)E_{01}(z_1-z_2)\ . \tag{4.24}$$

The total energy is obtained by solving the secular equation $\det|H_{ij}-E\delta_{ij}|=0$, which yields for the lowest energy state

$$E=\tfrac{1}{2}(H_{11}+H_{22})-\tfrac{1}{2}[(H_{11}-H_{22})^2+4H_{12}^2]^{1/2}\ . \tag{4.25}$$

As n increases, more configurations are mixed and the equations become more complicated. We don't consider them any further. In Fig. 2 we summarize our calculations for H_2 using the three different methods discussed above. We see that the calculation that takes

configuration interaction into account does give the correct behavior of the total energy for large separation.

B. Infinite H molecular chain (H_∞)

We calculate the ground-state energy of an infinite molecular chain of hydrogen in a superstrong magnetic field using a variational method. For an infinite chain, which is always beyond saturation, the simplest model of a cylinder of uniform electron density gives [see Eq. (3.7) with the Z dependence restored or Ref. [27]] the energy per atom for a Z chain:

$$E=-0.390Z^{9/5}b^{2/5}\ (\text{a.u.})=-119Z^{9/5}B_{12}^{2/5}\ (\text{eV})\ . \tag{4.26}$$

Comparing the value $E\simeq -119$ eV (for $Z=1$ and $B_{12}=1$) with the ground-state energy of a H atom at $B_{12}=1$, $E_a\simeq -160$ eV (see Table I), we have $E>E_a$, which is qualitatively wrong (see Sec. III). Clearly, the most naïve calculation above is not sufficiently accurate to determine the possibility or the binding energy of a chain versus an atom at $B_{12}\sim 1$. (The uniform cylinder model is reliable, however, for higher field strengths; see Sec. III.) Therefore, a more robust variational calculation is needed to obtain the results for field strengths characterizing neutron-star surfaces.

Glasser and Kaplan [2] generalized the uniform cylinder model above by considering the quantized electron charge distribution in the perpendicular direction. However, they assumed a uniform electron population in different Landau orbitals. The effect they treated amounts to only a small change in the value of the constant in the Madelung energy expression (3.6), and therefore it is still insufficient to account for the binding of chains.

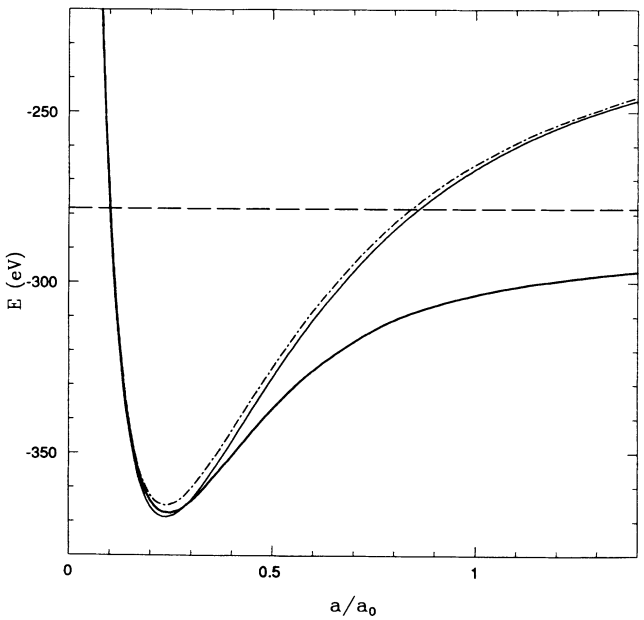

FIG. 2. The calculated energy of H_2 in a high magnetic field $B=10^{12}$ G as a function of the interatomic separation. The dot-dashed curve is from the MO calculation (Sec. IV A 1), the light solid curve is from the HF calculation (Sec. IV A 2), and the dark solid curve is from the MO calculation taking into account the configuration interactions (Sec. IV A 3). The dashed horizontal line corresponds to the sum of the energies of two separate H atoms, one in the ground state ($m=0$), another in the first excited ($m=1$): -161 eV -117 eV $=-278$ eV.

The next step in a more relaxed variational calculation is treating the effect of Coulomb potential on the population of electrons in different m orbitals [3]. This is clearly an important ingredient for calculating the binding of chains since it allows for more electrons in the inner orbitals (small m's), which increases the binding.

A further improvement in the calculation of chains includes the nonuniform electron density distribution in the z direction along the field [9]. This effect is important for treating the bound electrons (i.e., the "electron core" in [3]) correctly for chains of heavy atoms like $^{56}_{26}$Fe. But for light atoms such as H and He, the density variation along z is not significant since all the electrons in the chain are "ionized" and are well approximated by plane waves. A numerical comparison of a He chain with and without density variations along z indicates that indeed the variation can be safely ignored (see Sec. V).

For calculating a H chain, a variational calculation which assumes uniform density in the z direction is thus sufficient. This calculation is simpler than the full HF calculation of Neuhauser *et al.* [9] since the energy functional can be expressed in a semianalytic form. The calculation of Flowers *et al.* [3] contains numerical errors [4], indicating that this kind of calculation is subject to errors. Therefore, we are grateful that the mathematics we employ is a simplification of the reliable equations already derived by Neuhauser *et al.* [9].

1. Key equations

The basis electron wave functions are plane waves in the z direction with ground-state Landau orbitals in the perpendicular direction, i.e.,

$$\Phi_{mk}(\mathbf{r})=\frac{1}{\sqrt{L}}e^{ikz}W_m(\mathbf{r}_\perp)\ , \tag{4.27}$$

where $L=Na$ is the total length of the chain and k is the z wave-vector quantum number (the "Bloch wave vector"). Electrons fill the mth orbital (band) up to a Fermi wave number given by

$$k_m^F=\sigma_m\frac{\pi}{a}\ . \tag{4.28}$$

Here σ_m is the number of electrons in mth orbital per call. Charge neutrality demands

$$\sum_{m=0}^{m_0-1}\sigma_m=Z\ , \tag{4.29}$$

where Z is the nuclear charge (for a H chain, $Z=1$). Here m_0 is the number of occupied orbitals, i.e., $m=0,1,2,\ldots,m_0-1$.

We then obtain for the energy per cell in a chain

TABLE I. Interatomic equilibrium separation a (in units of $a_0=0.529$ Å) and binding energy *per atom* $|E|$ (in eV) for H_n molecules in a superstrong magnetic field. Binding energies for a H atom and the negative ion H^- are also given, together with the *total* binding energy and interatomic separation for the molecular ion H_2^+. B_{12} is the magnetic-field strength in units of 10^{12} G. Values in $(\cdots)$ are believed to give spuriously low binding energies; values in $[\cdots]$ for H_∞ at $B_{12}=500$ are calculated up to $m_0=12$ (see text).

B_{12}	H	H^-	H_2^+		H_2		H_3		H_4		H_∞	
(10^{12} G)	$\|E\|$	$\|E\|$	a	$\|E\|$	a	$\|E\|$	a	$\|E\|$	a	$\|E\|$	a	$\|E\|$
0.1	76.37	83.3	0.61	99.9	0.54	80.15	(0.48	77.07)	(0.46	71.75)	(0.58	79.04)
0.5	130.2	141.2	0.35	182.0	0.31	145.1	0.27	145.8	(0.25	140.6)	0.31	146.5
1.0	161.5	174.7	0.28	232.0	0.24	184.3	0.22	188.7	(0.20	185.0)	0.23	190.4
2.0	198.5	214.5	0.23	293.2	0.19	232.6	0.17	242.6	(0.15	241.7)	0.17	246.9
5.0	257.1	277.2	0.18	393.3	0.15	311.7	0.13	333.4	0.12	338.8	0.12	347.7
8.0	291.9	314.7	0.15	454.6	0.13	359.8	0.11	390.5	0.10	400.7	0.099	414.2
10	309.6	333.6	0.15	485.9	0.12	383.9	0.11	418.8	0.092	432.9	0.092	450.1
100	540.5	582.8	0.085	920.2	0.070	729.3	0.059	847.4	0.048	915.0	0.038	1060
500	763.0	819.7	0.060	1362	0.050	1070	0.043	1298	0.030	1454	[0.022	1920]

$$E=\frac{\hbar^2}{2m_e}\sum_m \sigma_m \tfrac{1}{3}\left[\sigma_m\frac{\pi}{a}\right]^2 + \frac{Z^2e^2}{a}\left[-\ln\left[\frac{2a}{\hat{\rho}}\right]+\gamma+\frac{1}{Z}\sum_m\sigma_m\psi(m+1) - \frac{1}{2Z^2}\sum_{m,m'}\sigma_m\sigma_{m'}Y_{mm'}\right]+E^{\rm exch} \quad (4.30)$$

(see Ref. [9]). Here ψ is the digamma function

$$\psi(m+1)=\psi(m)+\frac{1}{m}\ , \quad \psi(1)=-\gamma\ , \quad (4.31)$$

where γ is Euler's constant, $\gamma=0.577\ldots$. The function $Y_{mm'}$ is given by

$$Y_{mm'}=\sum_{s=0}^{m+m'} d_s(m,m')\psi(s+1)\ , \quad (4.32)$$

where the coefficients $d_s(m,m')$ are given in Appendix C. The exchange energy is given by

$$E^{\rm exch}=-\frac{e^2}{2a}\sum_{m,m'}\sigma_m\sigma_{m'}\int_{-\infty}^{\infty}dz\frac{\sin(\sigma_m\pi z\hat{\rho}/a)}{\sigma_m\pi z\hat{\rho}/a}\frac{\sin(\sigma_{m'}\pi z\hat{\rho}/a)}{\sigma_{m'}\pi z\hat{\rho}/a}E_{mm'}(z)\ , \quad (4.33)$$

where the function $E_{mm'}$ is given in Appendix C.

For a given lattice spacing a, the occupation numbers σ_m ($m=0,1,2,\ldots,m_0-1$) are varied to minimize the total energy E under the constraint (4.29). We increase m_0 until further increase in m_0 results in no change in the distribution, i.e., $\sigma_{m_0-1}=0$. Typically, m_0 lies between 6 and 10. The constrained variation $\delta E-\varepsilon_F\delta\sum_{m=0}^{m_0-1}\sigma_m=0$ yields

$$\varepsilon_F=\frac{\hbar^2}{2m_e}\left[\frac{\pi\sigma_m}{a}\right]^2+\frac{Z^2e^2}{a}\left[\frac{1}{Z}\psi(m+1)-\frac{1}{Z^2}\sum_{m'}\sigma_{m'}Y_{mm'}\right]-\frac{e^2}{a}\sum_{m'}\int_{-\infty}^{\infty}dz\cos(\sigma_m\pi z\hat{\rho}/a)\frac{\sin(\sigma_{m'}\pi z\hat{\rho}/a)}{\sigma_{m'}\pi z\hat{\rho}/a}E_{mm'}(z)\ . \quad (4.34)$$

Here ε_F is a constant Lagrange multiplier (Fermi energy) which must be determined self-consistently. The system (4.34) consists of m_0 equations for the m_0 unknown parameters σ_m plus the constant ε_F. It is solved together with Eq. (4.29) for these unknown quantities.

V. NUMERICAL RESULTS AND DISCUSSION

Our results for $n=2,3,4$ are obtained from the single-determinant Hartree-Fock method (Sec. IV A 2 and Appendix B). The recipe for solving the Hartree-Fock equations is as follows: For a given interatomic separation a, guess the trial wave functions f; calculate the potentials K and J from Eqs. (4.17) and (4.18), or (B14) and (B15); guess eigenvalues ε_m and boundary values of the wave functions; and use the standard shooting algorithm [29] to obtain the eigenvalues and new wave functions for Eq. (4.16) or (B13). New potentials K and J are then calculated and the whole process is repeated until convergence is achieved. Thus we obtain the total energy as a function of a; the equilibrium separation can be found by locating the energy minimum. For Eq. (4.16) or (B13), we integrate inwards starting from a point $z=z_{\rm max}$ far from the center. Shooting succeeds when the boundary condition at the center, $f_m'(0)=0$, and the normalization condition $\int_{-\infty}^{\infty}dz|f_m(z)|^2=1$ are satisfied. Numerically, the wave functions are determined on a grid with arithmetically increasing spacing from $z=0$ to $z=z_{\rm max}$. Typically, $z_{\rm max}\sim 60-100$ (in units of $\hat{\rho}$) is sufficient coverage for field strengths of interest. The number of grid points

varies between 100 to 200 for sufficient accuracy. For zero separation, our Hartree-Fock H_2 molecule calculation gives the He atomic binding energy (excluding the e^2/a term); similarly, the energy of H_3 at zero separation gives the energy of a Li atom, etc. These limits provide checks on our numerical results. Our resulting atomic binding energies agree with other HF result [7–9] to within $\sim 0.5\%$.

Our procedure for calculating the infinite H chain is as follows: For given a, guess a value for m_0 and solve for the σ_m's and ε_F from Eq. (4.34) subject to the constraint of Eq. (4.29). Once the occupation fractions σ_m's are obtained, they are substituted into Eq. (4.30) to get the energy. We then increase m_0 and redo the calculation. The process is repeated until convergence is obtained. Thus the binding energy versus a and the equilibrium atomic separation are obtained. As the field increases, the number of Landau orbitals m_0 needed for convergence also increases. For example, at $B_{12}=1$, $m_0=5$ is needed for convergence, while at $B_{12}=10$, only $m_0=8$ orbitals are occupied. In our calculation, we allow up to 12 Landau orbitals ($m_0=12$), which is sufficient for numerical convergence if $B_{12}<100$. Our results for the infinite chain at $B_{12}=500$ are obtained from an extrapolation based on the calculations done up to $m_0=12$.

Our code for calculating the infinite H chain can also be used to calculate an infinite He chain [$Z=2$ in Eqs. (4.29)–(4.34)]. Our He results agree with those of Müller (1984) [4] to at least three significant figures for $B_{12}=1$ and $B_{12}=10$. Comparing with the results of Neuhauser *et al.* (1987) [9], which allow for a nonuniform density distribution along the field direction, our results for He chain energies agree to within 0.8% (the agreement improves for higher field strength). For example, at $B_{12}=1$, the ground-state energy of a He atom is -575.3 eV while our He chain energy per atom is -595.5 eV (equilibrium spacing $a=5.7\hat{\rho}$), resulting in a cohesive energy of ~ 20 eV. By comparison, Neuhauser *et al.* give a chain energy of -600 eV ($a\sim 6\hat{\rho}$), resulting in a cohesive energy of ~ 25 eV. At $B_{12}=5$, the atomic energy is -958.8 eV, our chain energy is -1105 eV ($a=6.7\hat{\rho}$), and our cohesive energy is therefore 146 eV, while Neuhauser *et al.* give the chain energy of -1108 eV ($a\sim 6.6\hat{\rho}$) and a cohesive energy of $\simeq 149$ eV. We see that our approximate treatment of the infinite chain is sufficiently robust to determine reliably the cohesive energy of the He chain. For the lighter element H, the effect of any nonuniform electron distribution in the field direction is even smaller due to a weaker Coulomb force. Therefore we expect that our results for the H infinite chain, which has not been analyzed previously, to be even more reliable.

In Table I we present our HF results for H_n molecules with $n=2,3,4$ and $n=\infty$ at various field strengths. The equilibrium interatomic spacing and the binding energy per atom (equal to the total binding energy of the molecule divided by n) are given. We note that at small B field, as n increases, the binding energy per atom increases first, then decreases slightly. We consider this small decrease of binding energy as n increases as spurious. It comes from the approximations employed in our calculation, and not from our numerical integration. As discussed in Sec. IV A 3, when the total length of the molecule increases, different configurations become more and more mixed, and the single-determinant Hartree-Fock method without multiple configuration interactions begins to break down. Specifically, the electrons begin to acquire some probability of occupying the $\nu\neq 0$ states as saturation is approached (see Sec. III). Also, the fact that the calculated binding energy of the infinite chain is close to the binding energy of a finite molecule before saturation confirms our belief that the decrease in binding energy is spurious. We therefore put those values of binding energy that are believed to be spuriously low in parentheses. The actual binding energies of these molecules can be better estimated by interpolation between the reliably calculated binding energies of the smaller molecules and that of the infinite chain. Presumably, a more detailed calculation taking configuration interactions into account can be performed to remove the small discrepancy quoted above.

In Table II we compare the calculated parameters of a H_2 molecule in a high magnetic field with a molecule in zero field. The molecular zero-point energy for the vibrational motion along the field direction is also included in the Table. Within the Born-Oppenheimer approximation, the interatomic potential curve governing the relative motion of the ions is the total molecular electronic energy as a function of the atomic separation $E(a)$. We fit $E(a)$ to a parabolic curve around the equilibrium separation [i.e., the minimum of the $E(a)$ curve] and get the effective spring constant from the second derivative of $E(a)$ at the equilibrium point. Our quoted values for the molecular zero-point energy $E_0=\frac{1}{2}\hbar\omega_v$ is for a H_2 molecule consisting of two protons. The zero-point energies for molecules of other hydrogen isotopes can be easily obtained from the scaling law $\hbar\omega_v \propto M^{-1/2}$, where M is the reduced mass of the molecule. It can be seen that the molecular dissociation energy and the vibrational excita-

TABLE II. Properties of H_2 in a superstrong magnetic field compared with those in zero field.

B_{12} (10^{12} G)	Dissociation energy (eV)	a (a_0)	Zero-point energy E_0 (eV)
0	4.75	1.4	0.26
1	45.5	0.24	5.3
5	109	0.15	12
10	149	0.12	15
100	378	0.07	33
500	614	0.05	57

tion energy greatly increase in a high magnetic field, while the size of the molecule greatly decreases.

In Table III we give the energy release for various molecular formation processes as calculated from the data in Table I. These quantities are crucial for determining the relative molecular abundances in a neutron-star atmosphere.

The scaling with B of the binding energies in Tables I and III is of particular interest: For $b \simeq 426 B_{12} \gg 1$, the ionization potential I_1 of the neutral hydrogen atom has the form of $5(\ln b)^2 F$ (eV), where F is a slowly varying function of b. The numerical values of the expression $5(\ln b)^2$ are shown in Table III. We see that F is indeed a slowly varying function, but the various asymptotic relations obtained in Sec. III become accurate only for extremely strong fields, e.g., F will eventually approach $\simeq 13.6/5$, but only for $b \gg 10^7$. Asymptotically, the dissociation energy D_2 of the diatomic molecule, the sixth column of Table III, should be of the same form, but this is approached even more slowly, so that D_2 is appreciably less than I_1 for intermediate field strength. The binding energy per atom of an infinite chain should increase as $b^{2/5}$ in the asymptotic regime, so that D_∞ should eventually become much larger than both I_1 and D_2. Table III shows that these quantities are indeed are indeed comparable at $b \sim 10^5$.

For completeness, we also include our results for the molecular ion H_2^+ in Tables I and III. The binding energy and equilibrium atomic distance of H_2^+ can be easily obtained by solving Eqs. (4.6)–(4.9). Our binding energy for H_2^+ agrees with that of Brigham and Wadehra [18] to within 2% for $B_{12}=0.1$ and 1.

As we have discussed in Sec. II, a H atom in a high magnetic field can easily attract an electron to form a bound H^- ion. The H^- ion may, in principle, be important for determining the opacity in a neutron-star atmosphere. We include our Hartree-Fock calculation results for the *total* binding energy of H^- in Table I and the ionization energy of H^- in Table III. Our results for the binding energy of H^- agree with those obtained by Pröschel *et al.* [8]. In our HF calculation, we have not been able to find a bound state for H^{2-}, consistent with our discussion in Sec. II that the only bound negative H ion is H^-. As seen in Table III, the ionization energy of H^- is greatly increased in a strong magnetic field, as compared to its value of 0.75 eV for $B=0$. Nevertheless, the ionization potential is small compared to that for the H atom and to the dissociation energy of H_2. The abundance of H^- may thus be small.

A point regarding the three-dimensional H lattice is worth mentioning. Up to now, the only self-consistent calculation of the atom, one-dimensional infinite chain, and three-dimensional solid in a strong magnetic field is the calculation by Jones [10,11] for Fe using density-functional theory. Density-functional theory in a strong magnetic field has several intrinsic uncertainties, e.g., the correlation energy functional is not rigorously determined. Nevertheless, these calculations indicate that, for Fe, the infinite chain is not bound, and the three-dimensional Fe solid is only weakly bound (cohesive energy $\lesssim 1$ keV). In the case of H, the infinite chain is strongly bound, as we have shown. It is interesting to know the relative binding energy of the H infinite chain and the three-dimensional H solid. By placing a pile of parallel infinite chains in contact with each other, we can construct a three-dimensional lattice (e.g., body-centered tetragonal; see [11]). We can estimate the binding energy of this three-dimensional lattice with respect to breakup into separate one-dimensional chains by calculating the Coulomb interaction energy between different chains. We approximate the structure of the single chain by the simplest uniform cylinder model as discussed in Sec. III with the parameters given by Eq. (3.7). We then fix the charge distribution within the chains and set the chain-chain axial separation roughly equal to two times the chain cylindrical radius. The dominant contribution to the Coulomb energy comes from the interaction between the nearest-neighboring atoms (subcylinders). In the case of body-centered tetragonal lattice, each atom has eight nearest neighbors. We calculate the interaction of the atom with its neighboring atoms using a Monte Carlo integration method. For atoms far away from each other, we can use the classical quadrupole-quadrupole interaction formula for the energy, i.e.,

$$W=\frac{3Q^2}{16r^5}(3-30\cos^2\theta+35\cos^4\theta)\ , \tag{5.1}$$

where Q is the quadrupole moment of a subcylinder

TABLE III. Energy releases (in eV) from various atomic and molecular processes in a superstrong magnetic field. The values are calculated from the data in Table I. $b=B/(2.35\times10^9\ \mathrm{G})$.

B_{12} (10^{12} G)	$5(\ln b)^2$	Q (eV) $e+p=H$	$H+e=H^-$	$H+p=H_2^+$	$H+H=H_2$	$H_2+H=H_3$	$H_3+H=H_4$	$H_\infty+H=H_{\infty+1}$
0.1	70.2	76.4	6.93	23.6	7.56	3.78	3.78	3.78
0.5	144	130	11.0	51.8	29.8	17.0	15.6	16.3
1	183	161	13.2	70.5	45.6	36.0	27.2	28.9
2	227	199	16.0	94.7	68.2	64.1	44.1	48.4
5	293	257	20.1	136	109	120	97.9	90.6
8	331	292	22.8	163	136	160	139	122
10	349	310	24.0	176	149	179	166	141
100	568	541	42.3	380	378	543	577	520
500	753	763	56.7	599	614	991	1159	1157

$$Q=Q_{zz}=\int d^3\mathbf{r}_1\rho_e(\mathbf{r}_1)(3z_1^2-r_1^2)\ ,$$

r is the distance between two quadrupoles, and θ is the angle between the line joining the two quadrupoles and the z axis. We find that the resulting Coulomb energy is very small, less than 1% of the chain binding energy. This conclusion is certainly tentative, considering the approximations employed in our calculation are the sensitive dependence of the Coulomb integral on the chain-chain separation. Nevertheless, we expect that the binding energy of a three-dimensional H solid can be larger than that of a one-dimensional infinite H chain by not more than $\sim 5\%$.

VI. CONCLUSIONS

Strong magnetic fields are believed to exist on the surface and in the interior of many neutron stars. This magnetic field is not expected to affect the material structures deep inside the surface, where the matter density is high. When $\rho \gg 7.08\times 10^3\mu_e B_{12}^{3/2}$ (g/cm^3) [where μ_e is the mean molecular weight per electron and $B_{12}=B/(10^{12}$ G)], many Landau levels are filled by the electrons. In this regime, the quantized nature of the electron orbitals is smeared and the matter behaves like the material in a zero field (see, e.g., [26]).

On the surface of many neutron stars, on the other hand, the magnetic field B is strong and the matter density is relatively low, so almost all electrons are in their Landau ground states. Bound atoms, molecules, and chains may then be important and their existence in the neutron-star atmosphere may have some observable consequences for the observed x-ray spectrum from cooling and accreting neutron stars. For a neutron star with some accretion onto its surface (even if slow), the surface layers consist mainly of hydrogen and helium. The ionization-recombination equilibrium of atomic hydrogen depends mainly on the ratio $kT/(\ln b)^2$, where T is the temperature and b is the magnetic-field strength in units of 2.35×10^9 G. If the ratio is sufficiently small to give an appreciable abundance of neutral atomic hydrogen, at least diatomic molecular hydrogen can have a non-negligible abundance. For a fixed value of $kT/(\ln b)^2$, the long chains and solid hydrogen grains become more important in principle as b increases. However, if the field strengths are confined to $B_{12}\lesssim 10$, these larger structures are likely to have low abundance for the temperature regime of interest, $T\sim 10^5-10^6$ K. Since H_2 has many excited-state levels, some spectral lines may be observable or, if the collisional broadening should turn out to be strong, the neutron-star atmosphere opacities may be enhanced by the presence of H_2. We hope to investigate the molecular energy-level structure in the future.

ACKNOWLEDGMENTS

We thank Andrew Abrahams, Lars Bildsten, and David Chernoff for several useful discussions. This work was supported by NSF Grant Nos. AST 89-13112 and AST 90-15451 and by NASA Grant No. NAGW-2364 to Cornell University.

APPENDIX A: ANALYTICAL SCALING RELATIONS FOR H_n MOLECULES BEFORE SATURATION: VARIATIONAL CALCULATION

Before saturation, the n electrons occupy Landau orbitals $m=0,1,2,\ldots,n-1$. The radius of the molecular cylinder is $R\simeq\sqrt{2n/b}$. We assume $n\gg 1$. Our derivation for hydrogen molecules is similar to that of Kadomtsev and Kudryavtsev (1971) [24] for heavy atoms.

Ignore the exchange energy and define the average wave function $\Psi^2=n_e/n$, where the electron density is $n_e=\sum_{i=1}^{n}\Psi_i^2$. The total energy of the molecule then becomes

$$E=n\int d^3\mathbf{r}\left[\frac{1}{2}\left(\frac{\partial\Psi}{\partial z}\right)^2-\sum_{I=-n/2}^{n/2}\frac{1}{|\mathbf{r}-aI\hat{\mathbf{z}}|}\Psi^2+\frac{n-1}{2}\left\langle\frac{1}{r}\right\rangle\Psi^2\right]+\sum_{I<J}\frac{1}{|I-J|a}\ , \tag{A1}$$

where the four terms are electron kinetic energy, ion-electron interaction energy, electron-electron interaction energy, and ion-ion interaction energy, respectively. In the above equation,

$$\left\langle\frac{1}{r}\right\rangle=\int d^3\mathbf{r}_2\frac{1}{|\mathbf{r}-\mathbf{r}_2|}\Psi^2(\mathbf{r}_2)\ . \tag{A2}$$

Since the electron density has a sharp edge at radius R, in the direction perpendicular to the field, the electron density is well represented by a function of the form $e^{-\rho^2/R^2}$. We therefore take as a normalized trial wave function

$$\Psi^2(\mathbf{r})=\frac{\alpha}{\pi R^2}e^{-2\alpha|z|-\rho^2/R^2}\ , \tag{A3}$$

where α is the free variational parameter. Substituting the wave function into the energy expression (A1) and assuming $n\gg 1$, $\ln(1/\alpha R)\gg 1$, yields, to logarithmic accuracy,

$$E\simeq\frac{n\alpha^2}{2}-2n^2\alpha\ln\frac{1}{\alpha R}+\frac{1}{2}n^2\alpha\ln\frac{1}{\alpha R}+\frac{n}{a}\sum_{I=1}^{n/2}\frac{1}{I}\ . \tag{A4}$$

Equation (A4) can be obtained simply by considering the electron distribution as an average linear charge density $\lambda=\alpha\exp(-2\alpha|z|)$ and employing the radius R for the cutoff of any logarithmic divergence. For the second term in Eq. (A1), note that

$$\int d^3\mathbf{r}\frac{1}{|\mathbf{r}-aI\hat{\mathbf{z}}|}\Psi^2\simeq\alpha\int dz\frac{1}{|z-Ia|}e^{-2\alpha|z|}\simeq\alpha\int_{-1/\alpha}^{1/\alpha}dz\frac{1}{|z-Ia|}\simeq\alpha\left[\ln\left[\frac{1/\alpha-Ia}{R}\right]+\ln\left[\frac{1/\alpha+Ia}{R}\right]\right]\simeq 2\alpha\ln\frac{1}{\alpha R}\ , \tag{A5}$$

where we have used the cutoff R for z close to Ia. Thus we obtain the second term in Eq. (A4). For the third term in Eq. (A1), observe that $\langle 1/r\rangle$ can be regarded as the potential produced by the average linear charge distribution, which is equal to $2\lambda\ln(1/\alpha R)$. Accordingly, we have

$$\int d^3r\left\langle\frac{1}{r}\right\rangle\Psi^2\simeq\int dz\ 2\lambda^2\ln\frac{1}{\alpha R}=\alpha\ln\frac{1}{\alpha R}\ , \tag{A6}$$

which gives the third term in Eq. (A4).

The energy per atom is therefore

$$E/n\simeq\frac{\alpha^2}{2}+\frac{1}{a}\sum_{i=1}^{n/2}\frac{1}{i}-\tfrac{3}{2}(n\alpha)\ln\frac{n}{2}-\tfrac{3}{2}(n\alpha)\ln\frac{2}{n\alpha R}\ . \tag{A7}$$

Consider the second and third terms. For $n\gg1$, to make the sum of these two terms finite, we require

$$\frac{1}{a}=\tfrac{3}{2}n\alpha\ . \tag{A8}$$

With this condition, the sum of the second term and third term is $\frac{3}{2}n\alpha\gamma$ according to the relation

$$\sum_{i=1}^{n}\frac{1}{i}-\ln n\to\gamma\quad\text{as } n\to\infty\ , \tag{A9}$$

where $\gamma=0.577\ldots$ is Euler's constant. We then have

$$E/n=\frac{\alpha^2}{2}-\tfrac{3}{2}(n\alpha)\ln\frac{2}{n\alpha R}+\tfrac{3}{2}n\alpha\gamma\ . \tag{A10}$$

Varying E with respect to α gives, for $\ln(2/n\alpha R)\gg1$, a minimum value of E when

$$\alpha=\tfrac{3}{2}nl\ ,\quad E/n=-\tfrac{9}{8}n^2l^2\quad\text{for } l\gg1\ , \tag{A11}$$

where

$$l=\ln\frac{2}{n\alpha R}\simeq\ln\left[\frac{b}{n^5}\right]^{1/2}\ . \tag{A12}$$

Also from Eq. (A8), we see the interatomic separation is

$$a=\frac{4}{9n^2l}\ . \tag{A13}$$

This variational calculation gives the same results as our dimensional analysis in Sec. III.

APPENDIX B: HARTREE-FOCK EQUATION FOR H_n MOLECULES

The general Hamiltonian describing a linear H_n molecule with the ions lined up on the z axis along the B field is

$$H=H_B+V_{eI}+V_{ee}+V_{II}\ , \tag{B1}$$

where

$$H_B=\sum_i\frac{1}{2m_e}\left[\mathbf{p}_i+\frac{e}{c}\mathbf{A}_i\right]^2+\sum_i\frac{e}{m_ec}\mathbf{B}\cdot\mathbf{S}_i\ , \tag{B2}$$

$$V_{eI}=-e^2\sum_i\sum_I\frac{1}{|\mathbf{r}_i-Ia\hat{\mathbf{z}}|}\ , \tag{B3}$$

$$V_{ee}=e^2\sum_{i<j}\frac{1}{r_{ij}}\ , \tag{B4}$$

$$V_{II}=\frac{e^2}{2}\sum_{I\neq J}\frac{1}{|I-J|a}\ . \tag{B5}$$

In the equations above, a is ion spacing (we assume equal spacing); $\mathbf{S}_i$ is the electron spin; I,J label ions, i labels electrons, and $\mathbf{A}$ is the magnetic vector potential

$$\mathbf{A}=\tfrac{1}{2}\mathbf{B}\times\mathbf{r}\ . \tag{B6}$$

For all electrons in the ground Landau levels with spin aligned antiparallel to the B field, H_B reduces to

$$H_B=\sum_i\frac{1}{2m_e}p_{iz}^2\ . \tag{B7}$$

Choosing the trial function to be the antisymmetrized product of the basis functions

$$\Phi_{m\nu}(\mathbf{r})=W_m(\rho,\phi)f_{m\nu}(z)\ , \tag{B8}$$

we obtain

$$\begin{aligned}\langle H\rangle=&\frac{\hbar^2}{2m_e\hat{\rho}^2}\sum_{m,\nu}\int dz\,|f'_{m,\nu}(z)|^2-\frac{e^2}{\hat{\rho}}\sum_{m,\nu}\int dz\,|f_{m,\nu}(z)|^2\tilde{V}_m(z)\\&+\frac{e^2}{2\hat{\rho}}\sum_{m,\nu,m',\nu'}\int dz\,dz'D_{mm'}(z-z')|f_{m,\nu}(z)|^2|f_{m',\nu'}(z')|^2\\&-\frac{e^2}{2\hat{\rho}}\sum_{m,\nu,m',\nu'}\int dz\,dz'E_{mm'}(z-z')f_{m,\nu}(z)f_{m,\nu}(z')f_{m',\nu'}(z')f_{m',\nu'}(z)\ ,\end{aligned} \tag{B9}$$

TABLE IV. The direct interaction coefficients $d_s(m,m')$ as defined by Eq. (C8). We only list half of the coefficients $d_s(m,m')$ here; the other half can be obtained from the identity $d_{m+m'-s}(m,m')=d_s(m,m')$. We quote the numbers to six decimals.

		$d_s(m,m')$									
m	m'	$s=0$	$s=1$	$s=2$	$s=3$	$s=4$	$s=5$	$s=6$	$s=7$	$s=8$	$s=9$
0	0	1.0									
1	0	0.5									
1	1	0.5	0.0								
2	0	0.25	0.5								
2	1	0.375	0.125								
2	2	0.375	0	0.25							
3	0	0.125	0.375								
3	1	0.25	0.25	0							
3	2	0.3125	0.0625	0.125							
3	3	0.3125	0	0.1875	0						
4	0	0.0625	0.25	0.375							
4	1	0.156 25	0.281 25	0.0625							
4	2	0.234 375	0.156 25	0.015 625	0.1875						
4	3	0.273 438	0.039 063	0.117 188	0.070 313						
4	4	0.273 438	0	0.156 25	0.140 625						
5	0	0.031 25	0.156 25	0.3125							
5	1	0.093 75	0.25	0.156 25	0						
5	2	0.164 063	0.210 938	0.007 813	0.117 188						
5	3	0.218 75	0.109 375	0.031 25	0.140 625	0					
5	4	0.246 094	0.027 338	0.109 375	0.046 875	0.070 313					
5	5	0.246 094	0	0.136 719	0	0.117 188	0				
6	0	0.015 625	0.093 75	0.234 375	0.3125						
6	1	0.054 688	0.195 312	0.210 937	0.039 063						
6	2	0.109 375	0.218 75	0.0625	0.03125	0.156 25					
6	3	0.164 063	0.164 063	0	0.125	0.046 875					
6	4	0.205 078	0.082 031	0.041 016	0.109 375	0.003 906	0.117 188				
6	5	0.225 586	0.020 508	0.102 529	0.034 180	0.068 359	0.048 828				
6	6	0.225 586	0	0.123 047	0	0.102 539	0	0.097 656			
7	0	0.007 813	0.054 688	0.164 063	0.273 438						
7	1	0.031 25	0.140 625	0.218 75	0.109 375	0					
7	2	0.070 313	0.195 313	0.125	0	0.109 375					
7	3	0.117 188	0.1875	0.023 437	0.0625	0.109 375	0				
7	4	0.161 133	0.131 826	0.002 930	0.118 164	0.017 578	0.068 369				
7	5	0.193 359	0.064 453	0.046 875	0.087 891	0.009 766	0.0976 656	0			
7	6	0.209 487	0.016 113	0.096 680	0.026 367	0.056 918	0.036 621	0.048 828			
7	7	0.209 473	0	0.112 793	0	0.092 285	0	0.085 449	0		
8	0	0.003 906	0.031 25	0.109 375	0.218 75	0.273 438					
8	1	0.017 578	0.095 703	0.195 313	0.164 063	0.027 344					
8	2	0.043 945	0.158 203	0.165 039	0.023 428	0.041 016	0.136 718				
8	3	0.080 566	0.183 105	0.071 777	0.012 207	0.118 164	0.034 180				
8	4	0.120 850	0.161 133	0.007 324	0.079 102	0.070 557	0.009 766	0.102 539			
8	5	0.157 105	0.108 765	0.008 057	0.017 666	0.005 493	0.076 294	0.036 621			
8	6	0.183 288	0.052 368	0.050 354	0.072 530	0.014 832	0.082 397	0.001 526	0.085 449		
8	7	0.196 381	0.013 092	0.091 644	0.021 148	0.063 446	0.028 839	0.048 065	0.037 384		
8	8	0.196 381	0	0.104 737	0	0.084 595	0	0.076 904	0	0.074 768	
9	0	0.001 953	0.017 578	0.070 312	0.164 063	0.246 093					
9	1	0.009 766	0.0625	0.158 203	0.1875	0.082 031	0				
9	2	0.026 855	0.119 628	0.176 269	0.071 777	0.002 930	0.102 539				
9	3	0.053 710	0.161 133	0.177 187	0.000 982	0.079 101	0.087 890	0			
9	4	0.087 280	0.167 846	0.040 283	0.030 518	0.102 661	0.005 493	0.065 918			
9	5	0.122 192	0.139 647	0.001 343	0.085 937	0.044 067	0.024 414	0.082 397	0		
9	6	0.152 740	0.091 644	0.013 092	0.097 015	0.001 007	0.077 362	0.019 073	0.048 065		
9	7	0.174 561	0.043 640	0.052 368	0.061 096	0.018 798	0.070 496	0.004 272	0.074 768	0	
9	8	0.185 471	0.010 910	0.087 280	0.017 456	0.061 096	0.023 498	0.046 997	0.029 907	0.037 384	
9	9	0.185 471	0	0.098 190	0	0.078 552	0	0.070 495	0	0.067 291	0

where

$$\tilde{V}_m(z)=\int d^2\mathbf{r}_\perp |W_m(\mathbf{r}_\perp)|^2 \sum_I \frac{1}{|\mathbf{r}-Ia\hat{\mathbf{z}}|}=\sum_I V_m(z-Ia)\ , \tag{B10}$$

$$D_{mm'}(z_1-z_2)=\int d^2\mathbf{r}_{1\perp} d^2\mathbf{r}_{2\perp} |W_m(\mathbf{r}_{1\perp})|^2 |W_{m'}(\mathbf{r}_{2\perp})|^2 \frac{1}{r_{12}}\ , \tag{B11}$$

$$E_{mm'}(z_1-z_2)=\int d^2\mathbf{r}_{1\perp} d^2\mathbf{r}_{2\perp} W_m(\mathbf{r}_{1\perp}) W_{m'}(\mathbf{r}_{2\perp}) W_m^*(\mathbf{r}_{2\perp}) W_{m'}^*(\mathbf{r}_{1\perp}) \frac{1}{r_{12}}\ . \tag{B12}$$

(For some useful mathematical formulas related to the functions V_m, $D_{mm'}$, $E_{mm'}$, see Appendix C). Varying $\langle H\rangle$ with respect to f, we get the Hartree-Fock equations

$$\left[-\frac{\hbar^2}{2m_e\hat{\rho}^2}\frac{d^2}{dz^2}-\frac{e^2}{\hat{\rho}}\tilde{V}_m(z)+\frac{e^2}{\hat{\rho}}K_m(z)-\varepsilon_m\right] f_m(z) = \frac{e^2}{\hat{\rho}} J_{m\nu}(z)\ , \tag{B13}$$

where

$$K_m(z)=\sum_{m',\nu'} \int dz' f_{m'\nu'}(z')^2 D_{mm'}(z-z')\ , \tag{B14}$$

$$J_{m\nu}(z)=\sum_{m',\nu'} f_{m',\nu'}(z)\int dz' f_{m'\nu'}(z') f_{m\nu}(z') \times E_{mm'}(z-z')\ . \tag{B15}$$

APPENDIX C: USEFUL MATHEMATICAL RELATIONS FOR LANDAU WAVE FUNCTIONS

Here we summarize some of the mathematical relations needed for our numerical electronic-structure calculations (see [7,8,30] for further details). Our length unit here is the cyclotron radius $\hat{\rho}=(\hbar c/eB)^{1/2}$.

The averaged Coulomb potential defined by Eq. (2.8) is

$$V_m(z)=\frac{1}{\sqrt{2}m!}\int_0^\infty \frac{x^m e^{-x}}{\sqrt{x+(z/\sqrt{2})^2}}dx\ . \tag{C1}$$

One may use a standard quadrature algorithm (e.g., Romberg integration; see [29]) to obtain the functions $V_m(z)$. We do this for $3\le z\le 30$. Alternatively, for small z ($z\lesssim 3$), it is easier to relate it to the erfc functions by using a generating function

$$V(z,t)=\sum_{m=0}^\infty (1-t)^m V_m(z) = \left[\frac{\pi}{2t}\right]^{1/2}\exp\left[\frac{tz^2}{2}\right]\mathrm{erfc}(z\sqrt{t/2})\ , \tag{C2}$$

where

$$\mathrm{erfc}(x)=\frac{2}{\sqrt{\pi}}\int_x^\infty e^{-u^2}du\ . \tag{C3}$$

From Eq. (C2) for $V(z,t)$, we have

$$V_m(z)=\frac{1}{m!}\left[-\frac{d}{dt}\right]^m V(z,t)|_{t=1}\ . \tag{C4}$$

Therefore, we can obtain $V_m(z)$ from the erfc function. On the other hand, for large z ($z\gtrsim 30$), we can use the asymptotic expansion

$$V_m(z)=\frac{1}{|z|}\left[1-\tfrac{1}{2}(m+1)\left[\frac{\sqrt{2}}{z}\right]^2 +\tfrac{1}{2}\tfrac{3}{4}(m+1)(m+2)\left[\frac{\sqrt{2}}{z}\right]^4 -\tfrac{1}{2}\tfrac{3}{4}\tfrac{5}{6}(m+1)(m+2)(m+3)\left[\frac{\sqrt{2}}{z}\right]^6 +\cdots\right]\ . \tag{C5}$$

The electron-electron direct interaction kernel $D_{mm'}$ defined by Eq. (B11) and the exchange interaction kernel $E_{mm'}$ defined by Eq. (B12) can be shown to be related to the Coulomb interaction potential V_m by

$$D_{mm'}(z)=\sum_{s=0}^{m+m'} d_s(m,m')\frac{1}{\sqrt{2}}V_s\left[\frac{1}{\sqrt{2}}z\right]\ , \tag{C6}$$

$$E_{mm'}(z)=\sum_{s=0}^{m+m'} e_s(m,m')\frac{1}{\sqrt{2}}V_s\left[\frac{1}{\sqrt{2}}z\right]\ . \tag{C7}$$

The coefficients are defined by

$$L_m\left[\frac{x}{2}\right]L_{m'}\left[\frac{x}{2}\right]=\sum_{s=0}^{m+m'} d_s(m,m')L_s(x)\ , \tag{C8}$$

$$\frac{m!}{m'!}\left[\frac{x}{2}\right]^{m'-m}\left[L_s^{m'-m}\left[\frac{x}{2}\right]\right]^2=\sum_{s=0}^{m+m'} e_s(m,m')L_s(x)\ , \tag{C9}$$

where L_n^α is the Laguerre polynomial of order n [31]. Hence the coefficients d and e share the properties of the Laguerre polynomials. We can calculate these coefficients from the orthogonal relations of Laguerre polynomials. In Table IV we give the coefficients $d_s(m,m')$ for $m,m'\le 9$. The exchange coefficients $e_s(m,m')$ as defined in Eq. (C9) are related to $d_s(m,m')$ by the relation

$$e_s(m,m')=(-1)^s d_s(m,m')\ .$$

[1] M. Ruderman, in *Physics of Dense Matter,* International Astronomical Union Symposium No. 53, edited by C. J. Hansen (Dordrecht, Holland, 1974).
[2] M. L. Glasser and J. I. Kaplan, Astrophys. J. **199**, 208 (1975).
[3] E. G. Flowers, J. F. Lee, M. A. Ruderman, P. G. Sutherland, W. Hillebrandt, and E. Müller, Astrophys. J. **215**, 291 (1977).
[4] E. Müller, Astron. Astrophys. **130**, 415 (1984).
[5] R. O. Mueller, A. R. P. Rau, and L. Spruch, Phys. Rev. Lett. **26**, 1136 (1971).
[6] A. M. Abrahams and S. L. Shapiro, Astrophys. J. **382**, 233 (1991).
[7] J. Virtamo, J. Phys. B **9**, 751 (1976).
[8] P. Pröschel, W. Rösner, G. Wunner, H. Ruder, and H. Herold, J. Phys. B **15**, 1959 (1982).
[9] D. Neuhauser, S. E. Koonin, and K. Langanke, Phys. Rev. A **36**, 4163 (1987).
[10] P. B. Jones, Mon. Not. R. Astron. Soc. **216**, 503 (1985).
[11] P. B. Jones, Phys. Rev. Lett. **55**, 1338 (1985); Mon. Not. R. Astron. Soc. **218**, 477 (1986).
[12] M. Ruderman and P. G. Sutherland, Astrophys. J. **196**, 51 (1975).
[13] C. Alcock and A. Illarionov, Astrophys. J **235**, 534 (1980).
[14] P. Haensel and J. L. Zdunik, Astron. Astrophys. **227**, 431 (1990).
[15] O. Blaes, R. Blandford, P. Madau, and S. Koonin, Astrophys. J. **363**, 612 (1990).
[16] W. Rösner, G. Wunner, H. Herold, and H. Ruder, J. Phys. B **17**, 29 (1984).
[17] V. K. Khersonskii, Astrophys. Space Sci. **98**, 255 (1984); **117**, 47 (1985).
[18] D. R. Brigham and J. M. Wadehra, Astrophys. J. **317**, 865 (1987).
[19] A. V. Turbiner, Pis'ma Zh. Eksp. Teor. Fiz. **38**, 510 (1983) [JETP Lett. **38**, 618 (1983)]; S. Basile, F. Trombetta, and G. Ferrante, Nuovo Cimento D **9**, 457 (1987).
[20] For nontrivial separation of center of mass in magnetic fields, see J. E. Avron, I. B. Herbst, and B. Simon, Ann. Phys. (N.Y.) **114**, 431 (1978); H. Herold, H. Ruder, and G. Wunner, J. Phys. B **14**, 751 (1981); P. Schmelcher, L. S. Cederbaum, and H.-D. Meyer, Phys. Rev. A **38**, 6066 (1988).
[21] L. D. Landau and E. M. Lifshitz, *Quantum Mechanics,* 3rd ed. (Pergamon, Oxford, 1977).
[22] C. Angelie and C. Deutch, Phys. Lett. **67A**, 353 (1978).
[23] L. Haines and D. Roberts, Am. J. Phys. **37**, 1145 (1969).
[24] B. B. Kadomtsev and V. S. Kudryavtsev, Pis'ma Zh. Eksp. Teor. Fiz. **13**, 61 (1971) [JETP Lett. **13**, 42 (1971)].
[25] B. B. Kadomtsev, Zh. Eksp. Teor. Fiz. **58**, 1765 (1970) [Sov. Phys.—JETP **31**, 945 (1970)].
[26] I. Fushiki, E. H. Gudmundsson, and C. J. Pethick, Astrophys. J. **342**, 958 (1989).
[27] M. Ruderman, Phys. Rev. Lett. **27**, 1306 (1971).
[28] J. C. Slater, *Quantum Theory of Molecules and Solids* (McGraw-Hill, New York, 1963), Vol. 1.
[29] W. H. Press, B. P. Flannery, S. A. Teukolsky, and W. T. Vetterling, *Numerical Recipes: The Art of Scientific Computing* (Cambridge University Press, New York, 1987).
[30] J. Virtamo and P. Jauho, Nuovo Cimento B **26**, 537 (1975).
[31] M. Abramowitz and I. Stegun, *Handbook of Mathematical Functions* (Dover, New York, 1972).